

Maria Marques and Rodrigo Tiosso

## BRAZILIAN MINERAL CLAY AS SUPPORT FOR METALLOCENE CATALYST IN THE SYNTHESIS OF POLYETHYLENE

Instituto de Macromoleculas Professora Eloisa Mano/UFRJ  
 Caixa Postal 68525, 21941-590 Rio de Janeiro  
 fmarques@ima.ufrj.br

Received: November 19, 2009

© Marques M., Tiosso R., 2010

**Abstract.** Silica was compared with clays as supports for metallocene. Ethylene homopolymerization with both homogeneous and heterogeneous catalysts was performed. Activation energy was higher for  $(n\text{-BuCp})_2\text{ZrCl}_2/\text{SiO}_2/\text{MAO}$ , although high activities were obtained for catalysts with clay. They showed  $E_a$  close to that of homogeneous precursor. Catalyst/clay control polymer morphology until 363 K.

**Keywords:** clay, support, metallocene catalysts, polyethylene, nanocomposite.

## 1. Introduction

The polymerization systems employing metallocene technology in solution have a lot of disadvantages, which limit their use in the current polyolefin production processes. The major disadvantages found for homogeneous metallocene catalysts are the lack of control over the morphology of the polymer particles formed and the deposition of polymer on the reactor walls [1-3]. Studies of metallocene catalyst heterogenization are currently being carried out to overcome this problem, by immobilizing the metallocene complex on adequate supports, such as magnesium chloride, silica, alumina, and zeolite, or mesoporous materials.

An important modification caused by catalyst heterogenization is the reduction of catalyst activity due to the partial deactivation and/or undesirable reactions among metallocene compounds and active sites on the support surface [4, 5].

Several studies show that using of other supports (with different textural and physical-chemical characteristics) or even changing of the catalyst preparation techniques while maintaining the same support type have a marked influence on the performance of catalyst systems [6-8].

In the present work two types of materials were used as support: bentonite clay and silica. Table 1 shows mineral clays of the smectite group that are generically called bentonite. Their most important characteristics are good swelling capacity (over 20 times of their initial volume); high surface area (over 800 m<sup>2</sup>/g); ion (*e.g.* cation) exchange capacity (CEC) from 60 to 170 meq/100 g and tixotropy [9].

The crystal structure of smectite consists of layers composed of two tetrahedral coordinated silicon atoms (SiO<sub>2</sub>) fused to an edge-shared octahedral sheet of either aluminum or magnesium hydroxide (Al<sub>2</sub>O<sub>3</sub> or MgO). The interlayer spacing (*d*-spacing) changes with the inner cation (R<sup>+</sup>), being 9.8 E (Na<sup>+</sup>) or 12.1 E (Ca<sup>2+</sup>), and water molecules are linked through Van der Waals forces. The interlayer expansion for calcium smectite is around 17 E and for sodium smectite it is about 40 E.

Table 1

Mineral clays of the smectite group and the respective chemical formulas [9]

Octahedral cation	Octahedral lamellar charge	Tetrahedral lamellar charge
Fe <sup>+3</sup>	–	Nontronite R <sup>+</sup> <sub>0.33</sub> Fe <sup>+3</sup> <sub>2</sub> (Si <sub>3.67</sub> Al <sub>0.33</sub> )O <sub>10</sub> (OH) <sub>2</sub>
Al <sup>+3</sup>	Montmorillonite R <sup>+</sup> <sub>0.33</sub> (Al <sub>1.67</sub> Mg <sub>0.33</sub> )Si <sub>4</sub> O <sub>10</sub> (OH) <sub>2</sub>	Beidelite R <sup>+</sup> <sub>0.33</sub> Al <sub>2</sub> (Si <sub>3.67</sub> Al <sub>0.33</sub> )O <sub>10</sub> (OH) <sub>2</sub>
Mg <sup>+2</sup>	Hectorite R <sup>+</sup> <sub>0.33</sub> (Mg <sub>2.67</sub> Li <sub>0.33</sub> )Si <sub>4</sub> O <sub>10</sub> (OH) <sub>2</sub>	Saponite R <sup>+</sup> <sub>0.33</sub> Mg <sub>3</sub> (Si <sub>3.67</sub> Al <sub>0.33</sub> )O <sub>10</sub> (OH) <sub>2</sub>

R<sup>+</sup> = inner cation

Table 2

Chemical composition of natural bentonite [9]

Sample	Al <sub>2</sub> O <sub>3</sub>	CaO	Fe <sub>2</sub> O <sub>3</sub>	K <sub>2</sub> O	MgO	MnO	Na <sub>2</sub> O	P <sub>2</sub> O <sub>5</sub>	SiO <sub>2</sub>	TiO <sub>2</sub>
BBFB	14.7	0.47	7.5	0.24	2.0	0.01	0.49	0.05	64.9	0.71

The Brazilian bentonite samples were collected in the city of Mina Brava, Paraiba. Some characterization analyses, such as X-ray fluorescence (XRF), X-ray diffraction (XRD) and cation exchange capacity (CEC), were performed [9].

Natural bentonite (BBFB) was separated in two particle sizes by sieving. Table 2 shows the chemical composition of the BBFB sample by X-ray fluorescence.

The sample analyzed by X-ray diffraction was rich in montmorillonite, one of the smectite group members. Commonly, the exchanged cations in the clay lamellar layers, using aqueous solution, are Na<sup>+</sup>, Ca<sup>2+</sup>, Mg<sup>2+</sup>, H<sup>+</sup>, K<sup>+</sup> and NH<sub>4</sub><sup>+</sup>.

The BBFB sample showed a cation exchange capacity of 74 meq/100 g. The other Brazilian bentonites analyzed showed a CEC ranging from 60 to 170 meq/100 g.

Mineral clays have been used as support for metallocene catalysts to produce olefin nanocomposites by *in situ* polymerization. Most of the references in the literature report the use of montmorillonite as a support for metallocene catalysts [10-14].

## 2. Experimental

### 2.1. Materials

In this work two types of supports for the metallocene catalyst bis(*n*-butyl-cyclopentadienyl) zirconium dichloride were employed: (1) thermally treated commercial silica gel, supplied by Grace Davison – Sylopol 948, with 309 m<sup>2</sup>/g specific area, particle size in the range of 28–84 μm, and (2) two different bentonite samples: bentonite *in natura* from Mina Brava, Boa Vista, Paraiba State (calcium type), used as received after thermal treatment, donated by CETEM (Mineral Technology Center), named Sm<sub>3</sub> (particle size: 90–150 μm), and commercial sodium bentonite (BET), BENTOGEL® PETRO, from Bentonisa do Nordeste S.A., Brazil, used as received after thermal treatment. The silica used as support material required heating at 673 K (2°/min) during 4 h. The clays were dried at 393 K under nitrogen flow for 24 h.

Methylaluminoxane (MAO in toluene) and bis(*n*-butyl-cyclopentadienyl) zirconium dichloride were supplied by Crompton GmbH, Germany, and used as received. White Martins Gases Industriais (Praxair), Brazil, supplied ethylene at petrochemical grade purity, which was further purified by passing through columns filled with an activated 4E molecular sieve and copper catalyst. Toluene was supplied by Ipiranga Petroquímica, Brazil, and used after

treatment through a 3E molecular sieve, followed by reflux and distillation under a dry nitrogen and sodium/benzophenone system. Hexane was supplied by Petroflex, Brazil, and used after passing through a 3E molecular sieve and after being bubbled with dry nitrogen during 1 h.

### 2.2. Catalyst Preparation

All operations were carried out under nitrogen, using the Schlenk technique. MAO was employed in the support pre-treatment (concentration 5 mmol Al/g) at room temperature during 12 h, followed by washing with toluene at 363 K to remove cocatalyst residue.

For the support impregnation, a solution of homogeneous bis(*n*-butyl cyclopentadienyl) zirconium dichloride – (*n*-BuCp)<sub>2</sub>ZrCl<sub>2</sub> – in hexane was employed. The catalyst solution was left in contact with the pretreated support. The metallocene concentration used was 0.05 mmol of homogeneous catalyst per gram of support. The suspension obtained was kept under magnetic stirring for approximately 12 h, and then dried in a fluidized bed under N<sub>2</sub> until reaching constant weight. The catalyst activity was calculated by considering 100 % Zr impregnation on the support.

### 2.3. Catalyst and Support Characterization

The supports were characterized according to their specific area ( $S_g$ ), average pore volume ( $V_p$ ) and pore diameter ( $D_p$ ), through N<sub>2</sub> physisorption at 77.3 K (ASAP Micromeritics, model 2010). Samples were treated at 393 K during 24 h under a vacuum below 10 mm Hg.  $S_g$  was calculated according to the Brunauer-Emmet-Teller method, and  $V_p$  and  $D_p$  (in the range of 2 to 100 nm) were calculated by the Barrett-Joyner-Halenda method, at adsorption.

X-ray diffraction (XRD) measurements were performed with a Rigaku Miniflex X-ray diffractometer equipped with a Cu-Kα generator ( $\lambda = 1.5418$  Å), scanning from 2 to 20° at 0.05 step, with generator voltage of 30 kV at the current of 15 mA. The XRD measurements were used to determine the crystalline phases of both commercial clays (Sm<sub>3</sub> and BET) as well as of the supported catalyst.

### 2.4. Polymerization Reactions

The prepared catalysts were evaluated through ethylene polymerizations at different temperatures under

2 bar ethylene pressure. The polymerizations were carried out in a Buchi glass reactor coupled to a magnetic stirrer. The homogeneous catalyst concentration in the reaction medium was 50  $\mu\text{M}$  and the Al/Zr molar ratio applied was 1000 (MAO). For the supported catalyst, 100 mg in 100 ml of hexane was used.

The reactor was filled with solvent under a nitrogen atmosphere, followed by cocatalyst injection. Ethylene was added and the catalyst was injected to start the polymerization. The reaction was stopped after 30 minutes by adding ethanol/HCl (5 %). The polymers were purified with ethanol and dried until constant weight.

## 2.5. Polymer Characterization

### 2.5.1. Thermal analysis (DSC)

The polymers thermal characteristics such as melting temperature ( $T_m$ ) and crystallinity degree ( $X_c$ ) were obtained by differential scanning calorimetry (DSC) using a Perkin-Elmer DSC-7 at the heating rate of 10 K/min. Approximately 3.0 mg of polymer sample was sealed in aluminum pans. The temperature was raised from 313 to 423 K at the rate of 10°/min under nitrogen atmosphere. The sample was kept for 10 min at this temperature to eliminate the heat history before cooling at the rate of 10°/min.

### 2.5.2. X-ray diffraction (XRD)

Wide-angle X-ray spectra were recorded with a Rigaku Miniflex X-ray diffractometer. The X-ray beam was nickel-filtered Cu-K $\alpha$  ( $\lambda = 1.5418 \text{ \AA}$ ) radiation operated at 30 kV and 15 mA. Corresponding data were collected from 2° to 10° at the scanning rate of 1°/min.

### 2.5.3. Infrared spectroscopy (FTIR)

Fourier transform infrared spectrometry (FTIR) was used to determine the concentration of terminal groups in the polymeric chains, and subsequently to estimate the molecular weights of the polymers obtained. The number-

average molecular weights ( $M_n$ ) were evaluated using a calibration curve obtained from polyethylene samples, with their molecular weights being predetermined by gel permeation chromatography (GPC). Incorporated comonomer content was calculated from the FTIR analysis, according to Faldi & Soares' method [4]. FTIR analyses of polymers were conducted in a Perkin-Elmer FT-IR apparatus operating in the range of 700–400  $\text{cm}^{-1}$ , 50 scans and resolution of 4 $\text{cm}^{-1}$ . Composites were tested in 50-mm thick films.

## 3. Results and Discussion

### 3.1. Textural Characterization of Supports

In order to evaluate the influence of MAO and (*n*-BuCp)<sub>2</sub>ZrCl<sub>2</sub> immobilization on the support structure, textural analyses were performed in some of the heterogeneous catalysts prepared. Table 3 shows the specific area ( $S_g$ ), average pore volume ( $V_p$ ) and pore diameter ( $D_p$ ) of four groups of these catalysts: Si-CAT, Sm<sub>3</sub>-CAT and BET-CAT. For comparison, the respective analyses of the thermal pre-treated supports are also shown.

The support with the highest specific area is silica, followed by sodium bentonite (BET), the one made of Sm<sub>3</sub> being the support with the lowest specific area.

A marked reduction in the specific area and an increase in the average pore diameter  $D_p$  were observed for the BET-CAT catalyst. This effect can be attributed to the stronger reaction of MAO with this support during pretreatment, with more accessible hydroxyl groups and H<sub>2</sub>O molecules inside its lamellae, since the *d*-space is larger than in the other smectite samples (Sm<sub>3</sub>). Possibly the particle surface microporous structure was destroyed and consequently  $D_p$  increased. However, this did not occur with the Si-CAT catalyst, where a strong effect on specific area was not observed after impregnation of the catalyst components. On the other hand, a reduction of porous volume ( $V_p$ ) and pore diameter ( $D_p$ ) was observed.

Table 3

**Specific area, average pore volume and pore diameter of the catalysts: supported on silica (Si), bentonites *in natura* (Sm<sub>3</sub>) and commercial bentonite (BET)**

Supports	$S_g, \text{m}^2/\text{g}$	$V_p, \text{cm}^3/\text{g}$	$D_p, \text{\AA}$
Si	256	2.00	166
Si-CAT	276	1.00	127
Sm <sub>3</sub>	92	0.18	90
Sm <sub>3</sub> -CAT	72	0.13	89
BET	66	0.04	93
BET-CAT	3	0.01	204

Note: the samples were previously dried at 393 K.

### 3.2. X-Ray Diffractometry

Fig. 1 shows X-ray diffractograms of the BET support and of the catalyst prepared using this support. The commercial bentonite (BET) has a diffraction angle  $2\theta$  of  $6.8^\circ$ , which corresponds to 13.0 Å  $d$ -spacing, according to Bragg's Law.

Catalyst impregnation on clay possibly caused the bentonite to increase its interlayer spacing. Moreover, a broadening of the clay basal peak was observed. This is very important to produce nanocomposites by *in situ* polymerization, due to the exfoliation of clay lamellae by the growing polymer chain. Fig. 2 shows a model of this possible partial clay exfoliation on the supported catalyst during the polymerization of ethylene by the growth of polymer chains.

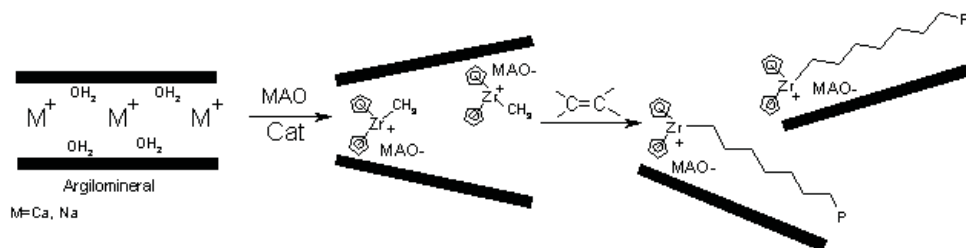


Fig. 2. Model of clay exfoliation during the polymerization with the metallocene supported catalyst

### 3.3. Catalyst Activity

#### 3.3.1. Effect of polymerization temperature

Ethylene homopolymerization using the homogeneous and heterogeneous catalyst systems studied was performed at three different temperatures (323, 343 and 363 K). Fig. 3 presents the results of catalyst activity for the homogeneous and heterogeneous metallocene systems.

The catalyst activity rose with the increase of polymerization temperature in the polymerizations using homogeneous catalyst. The highest activity was at 363 K.

Fig. 3b presents the polymerization results using the catalyst supported on silica. Comparing these reactions with those by the homogeneous counterpart, the activity of the silica supported system was much lower at 323 and 343 K, although at 363 K a sharp increase of catalyst activity was observed, achieving almost 4,000 ton PE/mol Zr·mol E·h.

In the polymerizations employing the catalyst system supported on bentonite *in natura*,  $\text{Sm}_3$  (Fig. 3c), there was also an increase in catalyst activity with the increase of the reaction temperature, although at 323 and 343 K the performance of this catalyst was also lower in comparison with the homogeneous system under the same

conditions. However, the highest activity was obtained with the silica supported system at 363 K.

Finally, with the catalyst supported on BET (Fig. 3d), there was an increase in performance with higher reaction temperature, and all activities were higher than in case with the  $\text{Sm}_3$  support.

Comparing the systems supported on  $\text{Sm}_3$  and BET, according to their catalyst activity, the BET support generated the highest activity at all polymerization temperatures, possibly because it contains a higher amount of active sites.

### 3.4. Polymer Characterization

#### 3.4.1. Thermal analysis (DSC)

Polyethylenes synthesized with the homogeneous catalytic system have sharply decreased melting temperatures ( $T_m$ ) with increasing reaction temperature. This is due to higher amount of branching in their chain because of the higher frequency of chain transfer reactions at increased polymerization temperature. Moreover, the  $T_m$  temperatures of the PEs synthesized employing the catalyst supported on silica were higher than those of polymers obtained by the homogeneous system (Fig. 4), and the

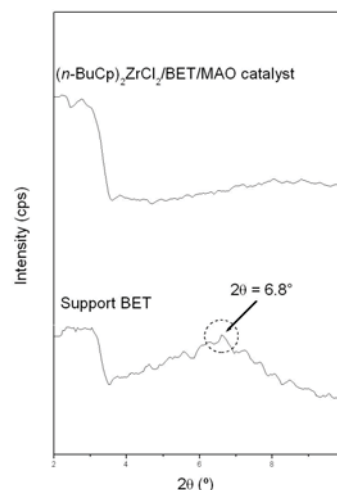
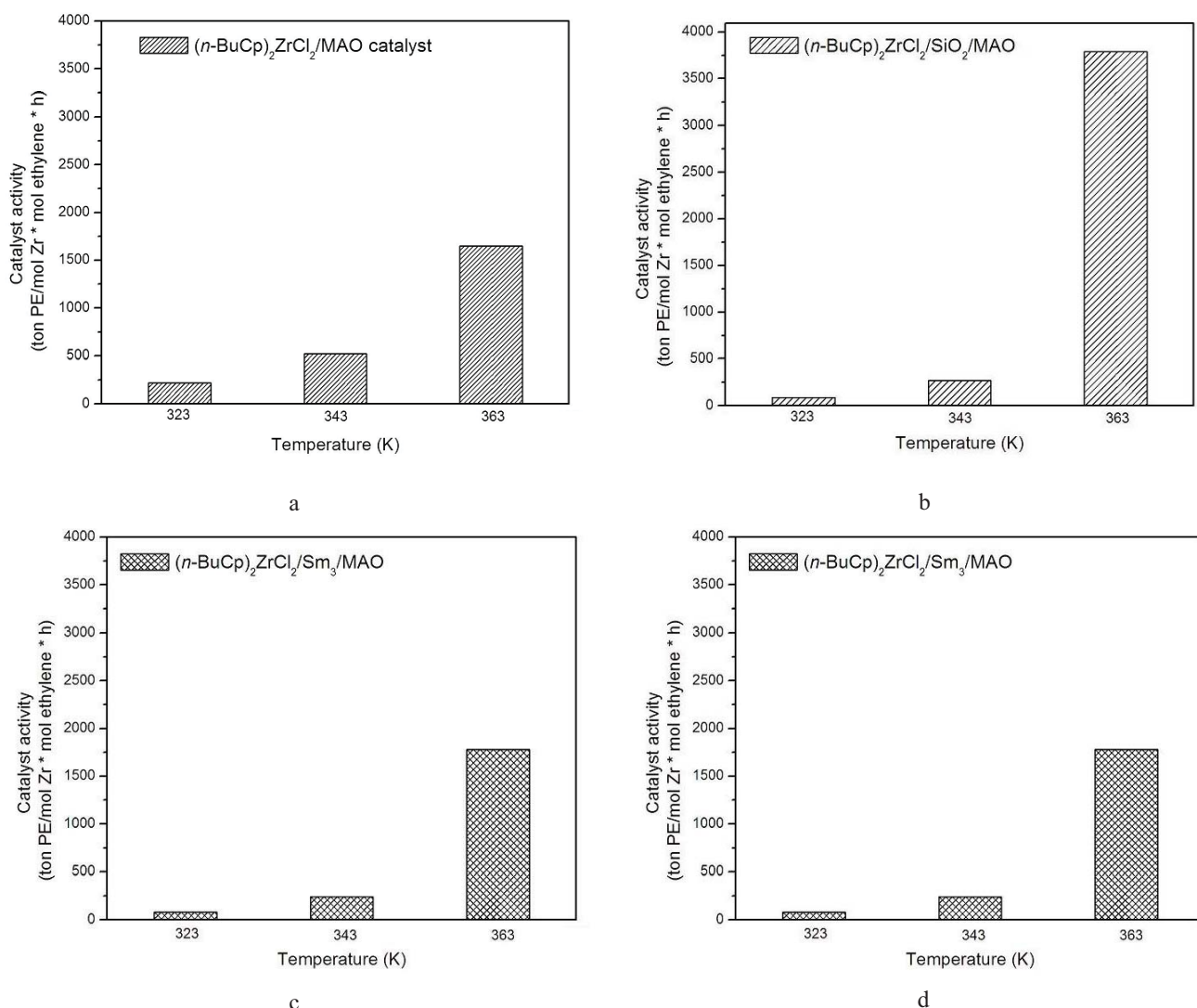


Fig. 1. Diffractograms of sodium bentonite support (BET) before and after MAO pretreatment followed by metallocene complex impregnation



**Fig. 3.** Ethylene polymerization with catalyst system  $(n\text{-BuCp})_2\text{ZrCl}_2/\text{MAO}$ : homogeneous catalyst (a); supported on silica (b); supported on  $\text{Sm}_3$  clay (c) and supported on BET clay (d)

effect of decreasing  $T_m$  with polymerization temperature was much lower. This effect of the supported catalysts is due to the sterical hindrance imposed by the solid surface, which causes low rates of chain transfer reactions.

The melting temperatures for the catalytic systems  $(n\text{-BuCp})_2\text{ZrCl}_2/\text{Sm}_3/\text{MAO}$  and  $(n\text{-BuCp})_2\text{ZrCl}_2/\text{BET}/\text{MAO}$  also decreased with increasing polymerization temperature. The highest melting temperatures were obtained with the use of  $\text{Sm}_3$  clay as support.

### 3.4.2. Infrared spectroscopy (FTIR)

A comparison of the PE results obtained with the homogeneous systems showed that the molecular weights were much smaller, even compared with those PEs synthesized with the supported systems. This indicates that the proximity between the  $[\text{Zr}^+-\text{MAO}^-]$  ionic pair allows greater transfer of  $H-\beta$  with a consequent drop in  $M_n$ , especially at higher polymerization temperatures.

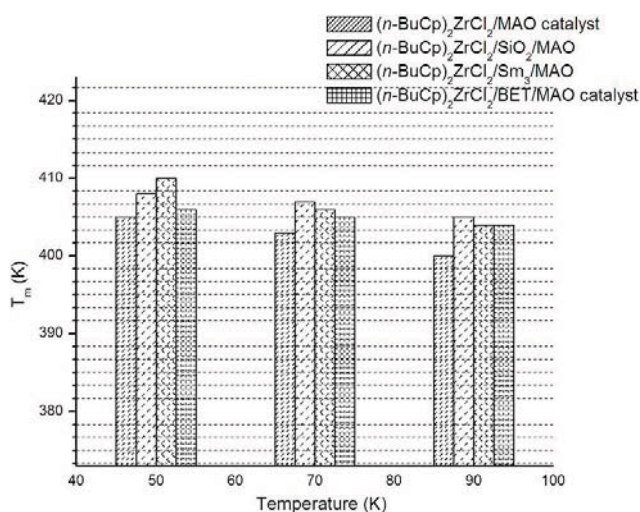


**Fig. 4.** Relation between melting temperature for homogeneous and heterogeneous catalysts at 323, 343 and 363 K

Table 4

Number-average molecular weight of polymers obtained by homogeneous catalyst as well as catalysts supported on silica, Sm<sub>3</sub> and BET and their respective normalized absorbances

Amostra	$T_p$ , K	$A_{965}/A_{4323}$ vinylene	$A_{908}/A_{4323}$ vinyl	$A_{888}/A_{4323}$ vinylidene	$M_n \cdot 10^{-3}$
HOM50	323	0.11	0.50	0.02	58.2
HOM80	353	0.34	2.52	0.05	12.6
Si50	323	0.06	0.08	0	256.1
Si80	353	0.08	0.44	0	70.8
Sm <sub>3</sub> 50	323	0.03	0.17	0	185.2
Sm <sub>3</sub> 80	353	0.30	0.79	0	34.2
BET50	323	0	0.16	0.02	206.1
BET80	353	0.20	0.67	0	42.3

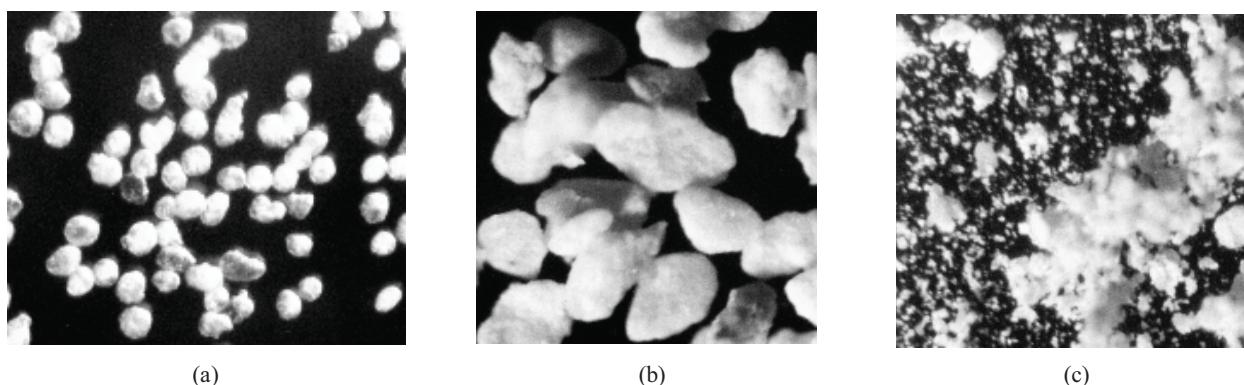


Fig. 5. Optical microscopy of the supports (x72): silica (a); Sm<sub>3</sub> *in natura* (b) and BET beneficiated bentonite (c)

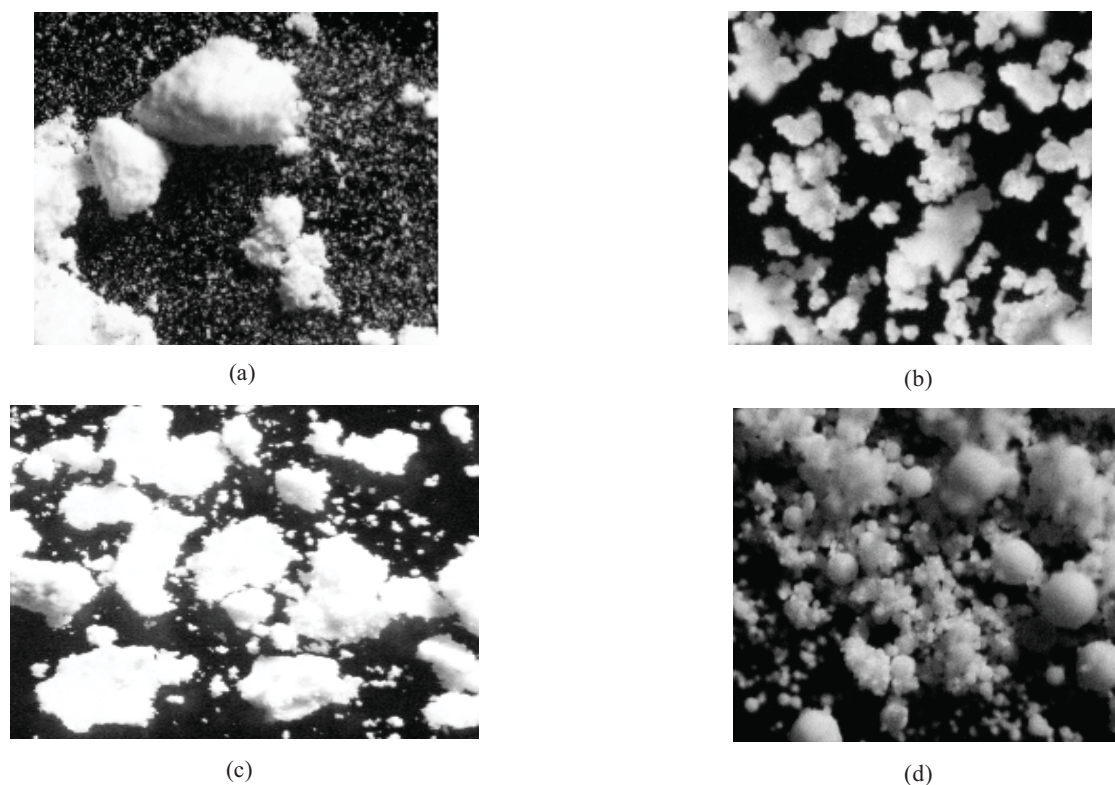


Fig. 6. Optical microscopy of polyethylenes obtained at 363 K with metallocene catalysts (x18): homogeneous (a); supported on silica (b); supported on Sm<sub>3</sub> clay (c) and supported on BET clay (d)

Therefore, there was a significant increase in the number-average molecular weight with heterogenization of the metallocene catalyst. The metallocene supported on silica produced PE with the highest molecular weight followed by sodium bentonite (BET).

The increase in temperature favored the formation of vinyl groups. In the vast majority of PE chain ends the presence of vinylidene groups was not observed.

### 3.4.3. Optical microscopy

Optical microscopy (OM) of both supports and the polymers synthesized with homogeneous ( $n\text{-BuCp}$ )<sub>2</sub>ZrCl<sub>2</sub> and supported catalyst systems was performed.

Fig. 5 shows OM micrographs of silica, Sm<sub>3</sub> and BET.

The Sm<sub>3</sub> particles are larger than the silica particles, although they are less spherical (Fig. 5b). On the other hand, sodium bentonite (BET) shows more irregular particles size distribution with higher numbers of particles with smaller size in comparison with both silica and Sm<sub>3</sub>.

The polyethylene produced with the homogeneous catalyst system at 363 K (Fig. 6a) shows poor morphology control with the presence of a lot of agglomerated as well as fine particles. On the other hand, the polymer synthesized with silica supported catalyst shows narrower particle size distribution and, most important, without fines, indicating better morphological control (Fig. 6b).

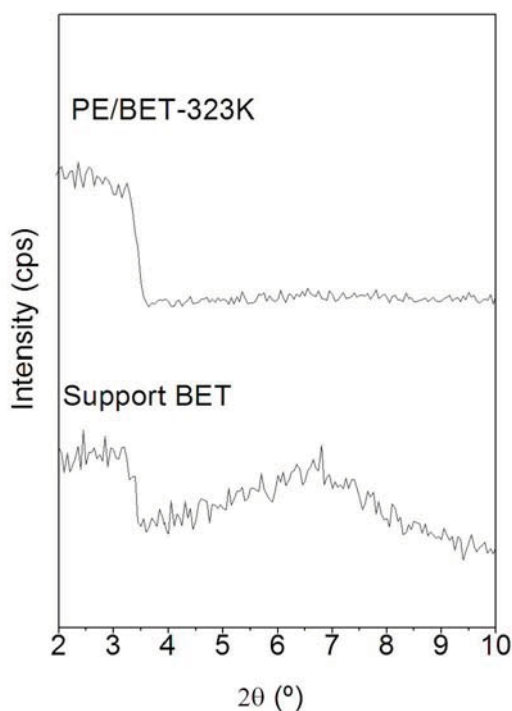


Fig. 7. Diffractograms of bentonite support (BET) and the polymer obtained at 323 K (PE-BET-323 K)

The polyethylene particles obtained with the clay Sm<sub>3</sub> support system are shown in Fig. 6c. The particles show some morphology control and no clay particles from the support can be visualized. However, fine particles are present, although the support particles are regular in size. Regarding the polymers obtained with the BET clay supported metallocene system shown in Fig. 6d, the morphology of the polyethylene seems to replicate that of the support, with larger size distribution, although without fines.

### 3.4.4. Polymer X-ray diffraction

Fig. 7 shows an X-ray diffractogram of polyethylene obtained with BET clay supported catalyst at 323 K compared with the BET support. It can be seen that the original clay presents a peak at around 7°, indicating an interlamellar distance of 1.26 nm. On the other hand, the HDPE/clay composite did not show X-ray diffractions at 2θ between 3.5° and 10°, indicating that the clay layer structure has changed, probably due to the increased distance between clay lamellae, so that the polymer chain promoted the intercalation or exfoliation of clay and produced a polyethylene nanocomposite.

## 4. Conclusions

Exfoliation of the clay layer was promoted by *in situ* polymerization of ethylene using Brazilian mineral BET clay supported ( $n\text{-BuCp}$ )<sub>2</sub>ZrCl<sub>2</sub> catalyst. The catalyst supported on BET clay was more active at 363 K than the other supported systems including the homogeneous one. The activation energy was higher for the silica-supported catalyst, and that of the clay supported catalyst was close to the homogeneous one. The melting temperatures of the polyethylenes obtained with the supported catalysts were higher than those with the homogeneous system. The optical microscopy of the support and the catalyst particles showed that the mineral clay with the largest particle size was fragmented during the catalyst preparation. On the other hand, the polymer morphology was controlled with the use of the employed supported systems. However, leaching of the active sites was observed in the reactions at 363 K using the catalyst supported on clay with the largest particle size.

## Acknowledgements

The authors are grateful to Fundacao Universitaria Jose Bonifacio-FUJB, Fundacao Carlos Chagas Filho de Amparo a Pesquisa do Estado do RJ -FAPERJ, and Conselho Nacional de Desenvolvimento Cientifico e Tecnologico-CNPq.

## References

- [1] Soga K., Arai T., Hoang B. and Uozumi T.: *Macromol. Rapid Commun.*, 1995, **16**, 905.
- [2] Hlatky G.: *Chem. Rev.*, 2000, **100**, 1347.
- [3] Ferreira M., Greco P., dos Santos J. and Damiani D.: *J. Mol. Catal. A*, 2001, **172**, 97.
- [4] Ribeiro M., Deffieux A. and Portela M.: *Ind. Eng. Chem. Res.*, 1997, **36**, 1224.
- [5] Fink G., Steinmetz B., Zechlin J. *et al.*: *Chem. Rev.*, 2000, **100**, 1377.
- [6] Marques M. and Moreira S.: *J. Mol. Catal. A*, 2003, **192**, 93.
- [7] Belelli P., Ferreira M. and Damiani D.: *Appl. Catal. A*, 2002, **228**, 189.
- [8] Lee K., Oh C., Yim J. and Ihm S.: *J. Mol. Catal. A*, 2000, **159**, 30.
- [9] Baltar C., Luz A., Oliveira C. and Aranha I.: [in:] *Caracterização, ativação e modificação superficial de bentonitas brasileiras*. CETEM, Rio de Janeiro 2003, 23-46.
- [10] Wang W., Fan Z. and Feng L.: *Eur. Polym. J.*, 2005, **41**, 2380.
- [11] Lee D., Kim H., Yoon K. *et al.*: *Sci. Technol. Adv. Mater.*, 2005, **6**, 457.
- [11] Liu C., Tang T. and Huang B.: *J. Catal.*, 2004, **221**, 162.
- [12] Shin S., Simon L., Soares J. and Scholz G.: *Polymer*, 2003, **44**, 5317.
- [13] Alexandre M., Dubois P., Sun T. *et al.*: *Polymer*, 2002, **43**, 2123.

**БРАЗИЛЬСЬКА МІНЕРАЛЬНА ГЛИНА ЯК НОСІЙ  
МЕТАЛОЦЕНОВОГО КАТАЛІЗАТОРА ПРИ СИНТЕЗІ  
ПОЛІЕТИЛЕНУ**

*Анотація.* Проведено порівняння кремнезему і глини як носіїв для металоцену. З використанням гомогенних і гетерогенних каталізаторів вивчено гомополімеризацію етилену. Встановлено, що енергія активації є вищою для  $(n\text{-BuCr})_2\text{ZrCl}_2/\text{SiO}_2/\text{MAO}$ , незважаючи на те, що каталізатори на основі глини мають більшу активність. Показано, що значення енергії активації є близькими для обох випадків. Співвідношення каталізатор/глина регулює морфологію полімеру до 363 К.

*Ключові слова:* глина, носій, металоценовий каталізатор, поліетилен, наноккомпозит.